Quantum and classical superparamagnetism in Stern-Gerlach simulation

Author: Marc de Paz Monfort
Advisor: Javier Tejada Palacios
Facultat de Física, Universitat de Barcelona, Diagonal 645, 08028 Barcelona, Spain.

Abstract: Many of the superparamagnetic classical and quantum phenomena can be observed with a Stern-Gerlach device, so the purpose of this TFG is to explore the behaviour of single domain particles in that device under certain conditions of temperature and magnetic field. A simulation is been performed in order to reproduce non analytical results. Some applications of the so mentioned experiment are also discussed.

I. INTRODUCTION

Single domain particles (SDP) are pieces of ferromagnetic crystals, which means with all its spins oriented parallel, whose size is small enough to make more energetically-costing to inverse one of its spins than to inverse the entire particle.
This allows us to treat them as huge-spin particles, due to their high exchange energy.

At the nanoscale, these super magnets and their analogous, the molecular magnets as Mn12 [1], [2], have contributed to the discovering of many quantum magnetic phenomena, such as tunnel effect and experimental observation of magnetic relaxation [3].

They also constitute one of the best new investigation lines to test quantum theories. In addition, they are expected to offer a great number of applications, including non-invasive nor radiological cancer treatment via tumour superheating and many other biomedical applications [4], manufacturing of quantum bits (qubits) and the improvement of the existing magnetic devices as magnetic bands, informatic memories, etc.

Additionally, SDP are an important future bet to investigate new theories at the frontiers of the science as they act as a bridge between classical and quantic worlds. Despite this, nowadays most of those applications are strongly limited because of the fact that a very narrow-peaked distribution is required.

The main goal of this work is to assess one of the purposed methods that uses a Stern-Gerlach device in order to filter an initial distribution and make it narrower. Stern and Gerlach, with their eminent experiment, made it undeniable the existence of a fourth degree of freedom at the quantum system of an atom, the spin.

By flying Ag atoms through a magnetic field gradient zone, the expected outcome of the experiment was a continuous stain due to the continuity of the electronic angular momentum, according to classical theory. Instead of it, two symmetric stains were obtained, revealing that Ag atoms had only two possible deflections, which meant the passage from the continuous to the discrete. SDP, on the other hand, are susceptible to change their quantic state due to thermal excitation.

This capability depends on spin and can be profited by the Stern-Gerlach device to acquire narrower distributions than current available.

II. MATHEMATICAL SUPPORT

It is known that a SDP immersed in a magnetic field at a certain temperature can flip between the parallel and the anti-parallel states due to thermal excitation. The characteristic time lapse in which this occurs is described by Néel's relaxation time law [3]

$$\tau_N = \tau_0 \cdot e^{\left(\frac{Ds^2}{K_b T}\right)} \qquad (1)$$

with τ_0 being the so called trial time and D being the anisotropy constant of the material. When the conditions of the experiment make this time lapse comparable with the time that a SDP takes to cross the magnetic field gradient zone, unblocking is observed.

As the Schrödinger equation exhibits no analytical solution for this system, [5] numerical solutions must be performed. Another possibility is to assume a certain model and simulate it instead.

In this TFG, the chosen model assumes that the SDP has an effective spin that is the expected value of all its possible projections weighted by its survival time [3].

$$s_{eff} = s \cdot \tanh\left(\frac{b_z s}{k_B T}\right) \qquad (2)$$

where $b_z = B_z g_s \mu_B$ is the second term of the Hamiltonian $H = -Ds_z^2 - b_z s_z$. As the SDP is moving on a non-uniform magnetic field this effective spin depends on its z position, and its z position depends on the effective spin. Then, the aim of the simulation is to measure the effective b_z factor.

Once b_z factor is known, the effective third component spin of a certain SDP is set, and so the expected value of its impact point on the collecting screen, for a given temperature.

This is the key information in order to use the Stern-Gerlach device as a classifier. A certain initial distribution will spread out after flying throughout the Stern-Gerlach apparatus according to its effective spin. So, one could send a certain initial distribution of SDP through the Stern-Gerlach device at a high temperature and reject blocked particles, those that has been deflected the most. Then repeat the experiment at a temperature and reject unblocked particles, those that have been almost non-deflected. By repeating this process, a narrow-peaked distribution is achieved, no matter how the initial distribution was.

Electronic address: marcdepazstadorotea@gmail.com

There is another relevant issue during the temperature changing, the magnetic field. The presence or absence of a uniform magnetic field when cooling or heating the sample causes different initial populations, and the Stern-Gerlach device is sensitive to it, producing such many different results.

As the Figure 1 shows, the presence of a magnetic field along the easy-magnetization axis makes the anisotropy barrier asymmetric. Then, flipping from parallel orientation to anti parallel one is no longer equally time-costing than the flipping from the antiparallel orientation to the parallel one. In other words, there is a preferable state.

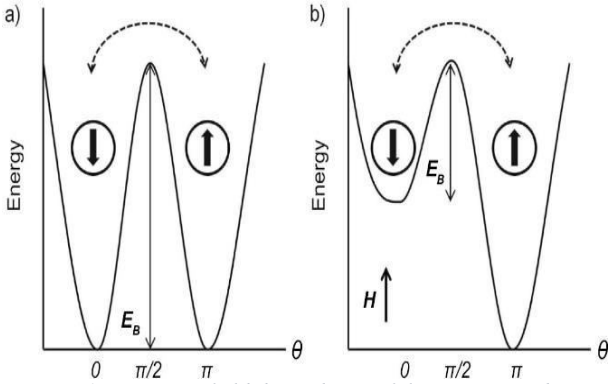

Figure 1: Magnetic field dependence of the anisotropy barrier.

If no magnetic field is set while cooling or heating, both parallel and antiparallel states are equally probable. This is also true in the very first income of the SDP into the Stern-Gerlach device. However, once the SDP starts deflecting, the magnetic field is not null, even with no external magnetic field. So, in the end, SDP have different probabilities to flip depending on the state they are.

In that experiment, this leads us to a distinction between the zero-field cooled and the field-cooled experiment as the field cooled will produce asymmetric stains.

As the antiparallel states have a lower barrier, the most stable state is the parallel one, so most of the SDP will behave as blocked particles with a parallel spin state and will produce a greater stain on the screen.

Regarding to tunnel effect, the Stern-Gerlach experiment with SDP can be used to observe it. The relevant parameter is again the temperature. When the very low temperature experiment is realized, only blocked behaviour is exhibited. Blocked particles' impact height is well known, so any other impact height must be the result of another mechanism for the spin to inverse and to act as an effective spin, that's tunnel effect.

If the magnetic barrier energy is higher than the thermic energy, thermal inversion is not permitted. Then the only way to inverse the spin of a SDP is by the tunnel effect. Then, splitting makes it possible for the spin to tunnel the barrier. Once the barrier is over, the spin is in an excited state, and will drop rapidly to the stable one.

Angular momentum conservation's law makes it impossible for the tunnel effect to occur unless a perpendicular magnetic field is set, making the energy of two different states equal. Otherwise, sz is an eigenstate of the Hamiltonian and it is conserved.

$$H = -Ds_z^2 - b_z s_z - b_\perp s_\perp \qquad (3)$$

The accuracy of the measurements of the tunnel effect increases with the decrease of the standard deviation of the spin sample. The more equal the SDP are the less noise in measurement we have, again due to thermal excitation.

The interesting thing is that a single device can process a desired sample and then make measurements. In addition, for certain materials, the lower required temperature is above 78 K, which is the boiling temperature of liquid nitrogen at atmospheric pressure. This makes the experiment possible with a relative cheap and simple cooling system.

III. DISCUSSION

A. METHOD

The chosen material for the simulation is a hypothetical one. In fact, all data was extracted from the Mn12 monomolecular magnet and SDP on this simulation are clusters of that molecules. The anisotropy constant is assumed to be the same than the Mn12, even knowing that now we have a cluster, not a single molecule. Then the material's parameters are the following:

Spin	Mass [a.m.u]	D [J]	D [eV]
10.0	1868.013516	$8.343121 \cdot 10^{-26}$	0,520737

Table 1: Material's parameters for the simulation.

The script starts by creating a sample with a gaussian distribution with μ=35 and σ=5. So, the average spin of the sample is 350. Once the initial population is created, initial third component of the spin is set, according to the presence or absence of a uniform magnetic field when cooling or heating.

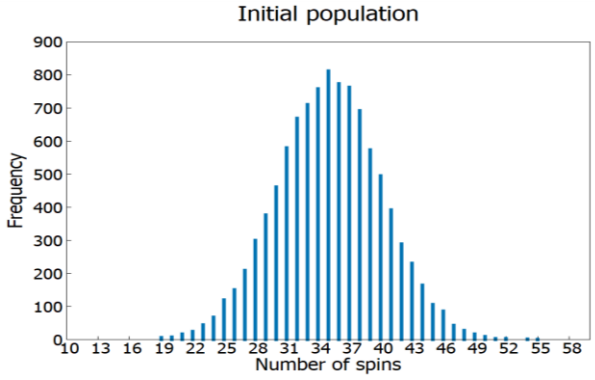

Figure 2: Initial population histogram.

Then, as previously mentioned, the entire sample is shot throughout the Stern-Gerlach device, particle by particle. During the flight, each particle has several opportunities of changing its third component of the spin. The probability of inversion is calculated as following [3]:

$$p(|s\rangle \rightarrow |-s\rangle) = \frac{1}{1 + e^{\frac{H - H_{max}}{k_B \cdot T}}} \qquad (4)$$

Once all particles reach the collecting screen, filtering is performed automatically by the computer. The height at which the filtering is done can be modified, but a bad value

will only cause the program to lengthen the computing time by increase its required iterations.

Two uncertainty sources are considered. The first one is the uncertainty due to a non-ideal collimator. This one causes the initial vertical speed not to be zero, but it can be taken into account using the uncertainty propagation method:

$$\delta z_{screen} = h_c \cdot \left(1 + \frac{l_{sg} + l_s}{l_c}\right) \qquad (5)$$

where h_c is the eight of the collimator, l_c its longitude, l_{sg} the longitude of the Stern-Gerlach device and l_s the distance between the end of the Stern-Gerlach device and the collecting screen.The considered values of those quantities and other ones referring to the geometry of the experiment are displayed on the following table

h_c [µm]	l_c [m]	l_{sg} [m]	h_{sg} [m]	l_p [m]	v_x [m/s]
1.00	1.00	0.20	0.10	2.00	100.00

Table 2: Device's parameters for the simulation. h_{sg} is the semi-height of the Stern-Gerlach device and v_x is the initial horizontal component of the velocity at which particles are shot.

The second uncertainty source is the computational randomness in each inversion trial. To assess it, initially identical experiments are launched, and the impact height uncertainty is taken as the standard deviation of those different experiments. The first uncertainty source has nothing to do with the conditions of the experiment, such as temperature or constant magnetic field. However, this second source depend explicitly on temperature. This is the reason why it must be calculated for each particle at every experiment, increasing considerably the simulating time.

In spite of this, it also offers output data, which are the basis for the simulation's goodness evaluation. From the equation (1), one can derive an expression for the trial time:

$$\tau_0 = \tau_N \cdot e^{-\left(\frac{Ds^2}{K_b T}\right)} \qquad (6)$$

As previously mentioned, unblocking occurs when τ_N is comparable to the flight time, $ft = \frac{l_{sg}}{v_x}$. The shape of the uncertainty function reveals two interesting facts. First of all, blocking, which is found because above a certain value for the spin, the uncertainty is almost zero ($\delta z \sim 10^{-17} m$). This can be used to calculate τ_0 knowing the first blocked spin.

The second fact is that a maximum is observed. This can be used to determine the most conflictive spin value. Performing the same calculation, another parameter can be extracted, τ_0'.

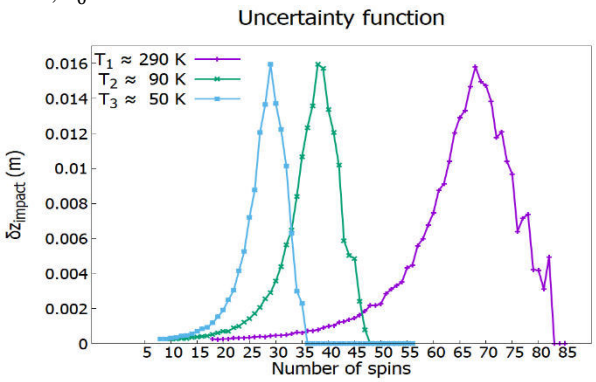

Figure 3: Uncertainty dependence on the spin for different temperatures.

In this case, the calculated values for τ_0 and τ_0' are the following:

	T_{low} (~50 K)	$T_{initial}$ (~90 K)	T_{high} (~280 K)
τ_0 ($\cdot 10^{-10} s$)	4.285	3.824	4.446
τ_0' ($\cdot 10^{-7} s$)	3.546	0.734	1.104

Table 3: Simulated output data.

Output data shows that the trial time has a reasonable value and, furthermore, that this value is approximately constant with temperature. In fact, the same single value for τ_0 reproduces quite well the blocking and the maximum uncertainty.

Once this parameter is known, random trials for the temperature are no longer needed as blocking temperature can be exactly computed, as well as blocking spin value.

$$T_B = \frac{D \cdot s^2}{k_B \cdot \ln\left(\frac{\tau_N}{\tau_0}\right)} \qquad (7)$$

$$N_B = \sqrt{\frac{k_B \cdot T}{D} \cdot \ln\left(\frac{\tau_N}{\tau_0}\right)} \qquad (8)$$

In order to obtain good results, the desired spin must be far away from the maximum uncertainty. Then, at low temperature, the desired spin should fall on the left queue of the uncertainty function and at high temperature it should be placed at the right queue. By imposing this condition, the low and high temperature values are set at 51 K and 285 K respectively. Notice that the almost-zero condition for the right queue ($\delta z \sim 10^{-17} m$) is much stronger than for the left one $\delta z \sim 10^{-5} m$. This fact, as explained below, is reflected on the final filtered population.

For the final analysis, one more issue must be discussed: the collecting grid. In order to reproduce the results as faithfully as possible in the actual experiment, finite detector element must be considered. Lower than the minimum uncertainty sized elements have no sense as they will tell nothing new. So, the size of the detecting elements is calculated for each temperature as the minimum uncertainty, and, also for esthetical reasons, it do change.

However, the minimum uncertainty corresponds to blocked particles and its value, $\delta z \sim 10^{-17} m$, has no practical sense as no detecting elements can be manufactured at that size. To avoid this problem, the script is equiped with a minimum reasonable value for the size of the detecting elements, $\delta z_{min} = 1 \cdot 10^{-6} m$. In spite of this, one of the goals for this simulation is to obtain the collecting height, and that does not depend on the size of the grid.

B. RESULTS

Once all the experiments are done, the program allows many data analysis. First of all, the impact density:

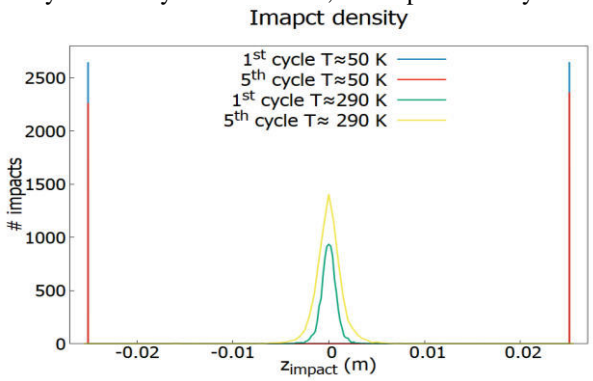

Figure 4: Impact density for different cycles at low temperature and high temperature.

Figure 4 shows that unblocked state is not so reliable as blocked. This is because once a particle unblocks, all its states are accessible and then it can behave as an effective-spin particle, so unblocked state is not well defined.

On the blocked plot, a reduction on impact density is observed. This is because non-normalized density is plotted. The reason for not plotting normalized density is because this way also the decrease of the population is shown. On the unblocked plot, decreasing is also occurring, but in this case, the effect of the temperature is higher. The higher maximum indicates that as more iterations are simulated, more particles exhibit unblocking behaviour. That's because every iteration is simulated at a lightly higher temperature than the previous one.

One other interesting analysis is to examine if there's correlation between the impact height and the spin of the SDP. Otherwise, filtering would result in useless process.

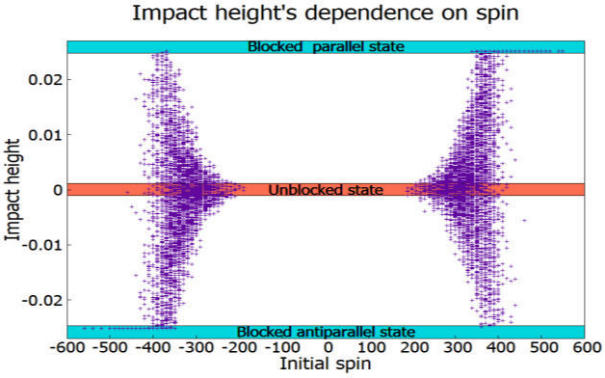

Figure 5: the graphic shows how the available impact heights depends on spin.

As figure 5 shows, there is no bijective relationship between spin and impact height for unblocked particles. Despite this, it does show the tendency for the small spins to behave as an almost-zero effective spin. This again has to do with the lack of reliability of the unblocked state in front of the blocked one. So, in this experiment, filtering will only eliminate the smallest particles at low temperature.

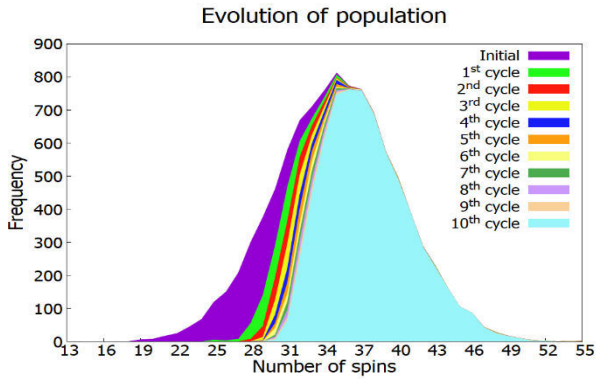

Figure 6: Evolution of the distribution with program iterations.

Results make it possible to evaluate the assumed model. Once the impact height is known por each particle, its experimental effective spin value can be computed as the one needed for a perfectly blocked spin to deflect the same angle. Then, adjusting the function from eq. 2 the effective magnetic field can be calculated.

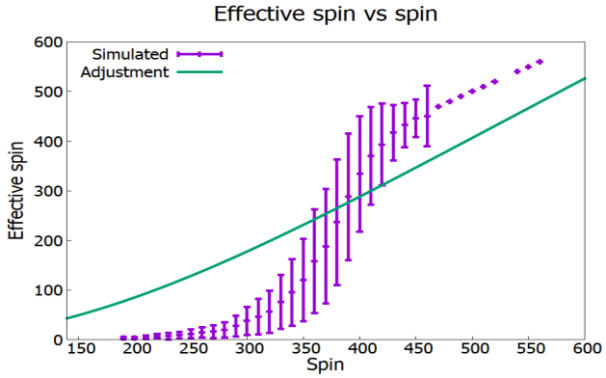

Figure 7: Model evaluation and output data obtention.

The adjustment offers a reasonable value for the effective magnetic field, $b_{z_{eff}} = 2.8 \pm 0.3 \cdot 10^{-24}\, J \rightarrow B_{z_{eff}} = \frac{b_{z_{eff}}}{\mu_B \cdot g_s} = 0.15 \pm 0.02\, T$, but as figure 7 shows, the behaviour of the SDP is not well reproduced. This tells us that probably the assumed model has some limitations.

The effect of setting a uniform magnetic field is appreciated in the following plots:

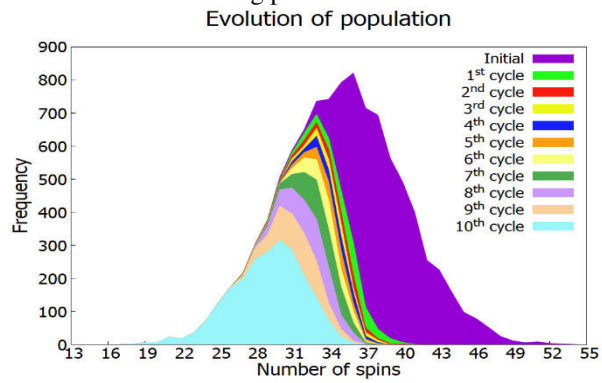

Figure 8: Evolution of the distribution with a constant magnetic field of B=2T applied.

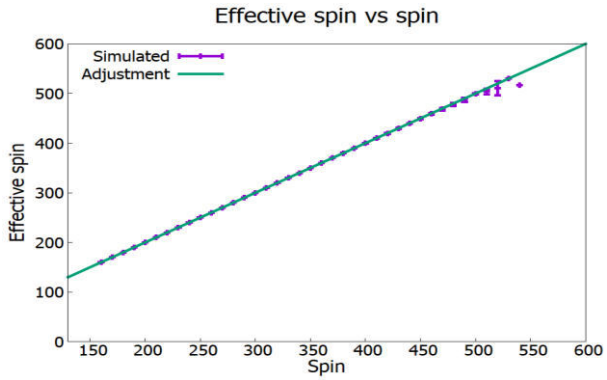

Figure 9: Model evaluation with a constant magnetic field of B=2T applied.

As figure 8 shows, the most highlighted effect of a uniform magnetic field is the filtering of high spin particles. This is because for a certain value of the magnetic field, the anisotropy barrier completely vanishes and the only stable state is the parallel one. So now, the smallest particles, which were previously unblocked, are now perfectly blocked on the parallel state as no other stable states are available.

Figure 9 tells about how good the model is for a high magnetic field. Now the great thing is that both experiments can be combined.

Now the great thing is that both experiments can be combined. One could perform the zero field cooled experiment in order to reject the smallest particles and then the field cooled experiment to refuse the largest ones. By simulating these experiments, the results shown on figure 10 can be achieved.

This figure is the evidence for the capability of the Stern-Gerlach device to narrow an initial SDP distribution with realistic values of temperature and magnetic field.

Zero standard deviation can be reached with this simulation, but it takes much time and the only benefit is knowing an approach of how many times the real experiment must be performed.

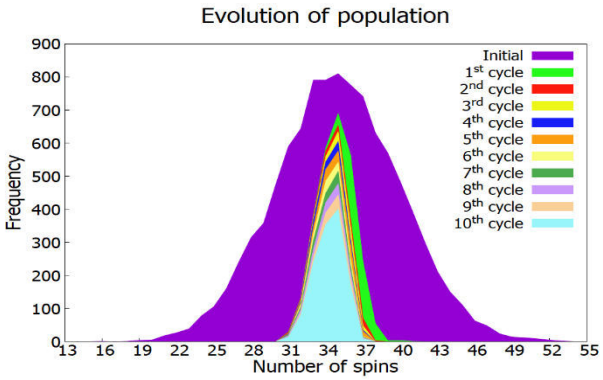

Figure 10: Evolution of the distribution combining zero and field cooled experiments with a magnetic field of B=1T.

IV. CONCLUSIONS

As the results of the simulation shows, the Stern-Gerlach device can effectively be used to obtain the narrow distributions needed for many of the SDP's applications with reasonable conditions. It is also observed that the effective spin model can reproduce well the behaviour of SDP at high magnetic field, but it has some limitations when trying to reproduce the unblocking behaviour at zero field.

Finally, the program is designed to enable the participation of other effects, such as tunnel effect, so it is a good issue to investigate about because of the improvements that the real experiment can make in our current technology.

V. Acknowledgments

To my advisor, Javier Tejada, for the commitment he has made to my academical growth and all the opportunities and support he has put on me. To my colleague, Aleix Bou, whose recommendations has made him imprescindible to make this work become a reality. To my family for making me believe in myself and encourage me in the worst moments and specially to my sisters Elisabet de Paz and Clara de Paz for helping me sharpen my mind and focus the minimum details. Finally, to my partner, Laia Ibern for the unconditional and imprescidible support, love and confidence she has brought to me along this entire journey.

[1] K.M.Mertes,Y.Suzuki,M.P.Sarachik,Y.Myasoedov H.Shtrikman E.Zeldov, et al. «Mn12-acetate: a prototypical single molecule magnet», Solid State Communications Vol. 127, Issue 2, July 2003, Pages 131-139

[2] J. Mejía-López y A. Mejía-López, «Propiedades magneticas en nanoestructuras» *Revista Cubana de Física*, vol. 34, No.1 pp. 80-87, 2017.

[3] Chudnovsky EM, Tejada J. Lectures on Magnetism with 128 problems. United States of America: Rinton Press; 2006.

[4] T. Neuberger, B. Schöpf, H. Hofmann,B. von Rechenberg, «Superparamagnetic nanoparticles for biomedical applications: Possibilities and limitations of a new drug delivery system», Journal of Magnetism and Magnetic Materials Vol. 293, Issue 1, Pages 483-496, May 2005.

[5] J. Daz Bulnes and I.S. Oliveira, «Construction of Exact Solutions for the Stern-Gerlach Effect», Brazilian Journal of Physics, vol. 31, no. 3, Pages 488-495 September, 2001